Identification of material model of TiN using numerical simulation of nanoindentation test

M. Kopernik*[1], A. Milenin[1], R. Major[2] and J. M. Lackner[3]

The development of the model of the multistep nanoindentation test with Berkovich indenter, accounting for the residual stress distribution, is one of the aims of the present paper. The specimen is unloaded in the intervals between the deformation steps. Substrate, which is composed of a ferritic steel and biocompatible pulsed laser deposition TiN coating, is considered. The selection of the TiN was inspired by its perspective application as the coating for a constructional element of the heart prosthesis (blood chamber and aortic valves). Sensitivity analysis of the model predictions with respect to its parameters is presented in the present paper. The theory of elastic–plastic deformations is used in the finite element model, which simulates both loading and unloading phases, accounting for the real geometry of the indent. The main goal of the present paper was to inversely analyse the tests for coating/substrate system. Square root error between measured and predicted forces is the objective function in the analysis. Results of the inverse calculations, which are presented in the present paper, may be helpful in simulations of the behaviour of TiN deposited on substrate in various applications as bionanomaterials.

Keywords: Nanoindentation test, Finite element method, Inverse analysis, TiN, Pulsed laser deposition, Residual stress

Introduction

The present work is part of a complex project with a general objective to simulate the mechanical behaviour of the systems of coatings, accounting for the new nanomaterials with increased biocompatibility introduced in Ref. 1. Numerical models of expected applications of these materials need the exact parameters of material model for all their layers. Knowledge about the real properties of nanomaterials, which are used for example in the constructional elements of the artificial heart prosthesis, is crucial for the accuracy of simulations. Coatings are tested in experimental nanoindentation tests because standard experimental methods performed in macroscale are not highly recommended by specialists for analysed case.

The experimental–analytical methods are mainly applied to monolayer materials, as presented in Ref. 2. Methods to estimate properties of the system of coatings are limited to the hardness and Young's modulus, as discussed in Refs. 3–5. However, these properties do not describe the complete material models of coatings. Owing to strong inhomogeneities of the tests, extracting these additional model parameters from the tests is difficult. Therefore, attempts towards the development of the finite element (FE) model of nanoindentation test, accounting for the residual stress distribution in the coating/substrate system, have been undertaken in the present work. This is a continuation of an earlier research presented in Ref. 6. That work was focused on recognising and overcoming various difficulties, which occur in the FE simulations of nanoindentation test for system of coatings using commercial FE codes.

It has been shown in Ref. 7, where carbon steel was investigated, that inverse analysis is an efficient and useful method of identification of material model on the basis of microindentation tests. These promising results inspired the authors to apply this method to the nanocoatings. Since the inverse analysis requires many simulations of the test and, moreover, due to scale problems, the simulation of nanocoatings is even more time consuming, the application of the commercial code would lead to a significant increase in the computation costs. Thus, two actions were undertaken in the present work. The FE code developed by the authors, which can easily be optimised and adjusted to distributed calculations, was adapted to the task of modelling of the nanoindentation test with residual stress distribution. Beyond this, the sensitivity analysis of the model output with respect to the model parameters was performed to evaluate importance of individual parameters and to select only those that have noticeable influence on the results.

Methodology and view from previous investigations

Identification of material properties for the TiN coating deposited by pulsed laser deposition (PLD) on ferritic

[1]Department of Applied Computer Science and Modelling, Faculty of Metals Engineering and Industrial Computer Science, AGH University of Science and Technology, Al. Mickiewicza 30, Kraków 30–059, Poland
[2]Institute of Metallurgy and Materials Science PAN (IMIM PAN), Ul. Reymonta 25, Kraków 30–059, Poland
[3]Leoben Laser Centre, Leobner Straße 94, Niklasdorf 8712, Austria

*Corresponding author, email magdalenakopernik@interia.pl

Published by Maney on behalf of the Institute
Received 23 December 2009; accepted 1 June 2010
DOI 10.1179/026708310X12756557336193

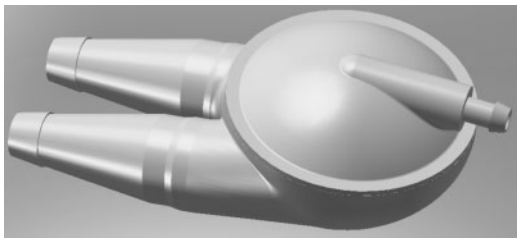

1 Artificial blood chamber[1]

steel is based on nanoindentation test. The main reason of applying PLD method described in Ref. 8 is possibility to deposit high chemical purity and good adhesive coatings on different substrates in low temperature (room temperature). In addition, the deposition process of coating in gas atmosphere allows to obtain thin films of a wide range stochiometry. The TiN coating is used, for example, for the demanding biotechnological applications because it increases the biocompatibility of the covered substrates (see Ref. 9). An artificial left blood chamber shown in Fig. 1 is an example of future application of this material, as discussed in Ref. 1. Authors have already performed simulations of artificial parts of heart prosthesis using the commercial FE code ADINA. A model of aortic valve developed in Ref. 10 is presented in Fig. 2. The opening phase of the process is shown. The calculated distribution of the effective stress on the outer surface of the open leaflet is presented in Fig. 3.

The three-dimensional (3D) FE model of the whole artificial heart chamber and local multiscale model was also developed by the authors.[11] Selected result of simulations using macromodel is shown in Fig. 4. Distribution of the average stress at the inner surface of the bottom part of the chamber in top view of the cross-section is presented.

Analysis of results in Refs. 10 and 11 confirms the model's good predictive capability, as far as qualitative aspects are considered. The quantitative accuracy depends, to a large extent, on correctness of selection of material parameters. Although the micromodel is locally adapted, the parameters for model of outer coating material are not realistic. Since the real material parameters of outer biocoatings are still unknown, purely elastic model was applied. As a consequence, the real behaviour of material under working conditions was not predicted with quantitative accuracy. Supplying

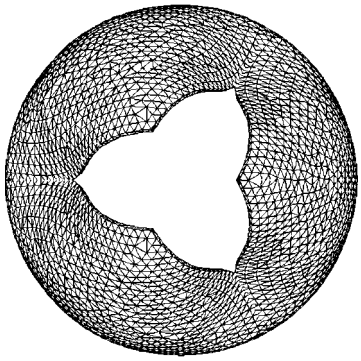

2 Model of aortic valve during opening process[10]

3 Distribution of effective stress computed[10] on outer surface of open leaflet

reliable material data was an objective of the present research.

The properties of outer coatings required for the specified applications (Martens hardness and Young's modulus) are studied in the two-stage nanoindentation tests. The consistency of experimental results is crucial for the identification of different characteristics of the deposited material. On the other hand, there are various disturbances in the experiment, which have an effect on the results. Moreover, the indenter is subjected to elastic deformation, which is difficult to evaluate. Thus, obtaining the complete material model of coatings directly from the tests is not possible or at least

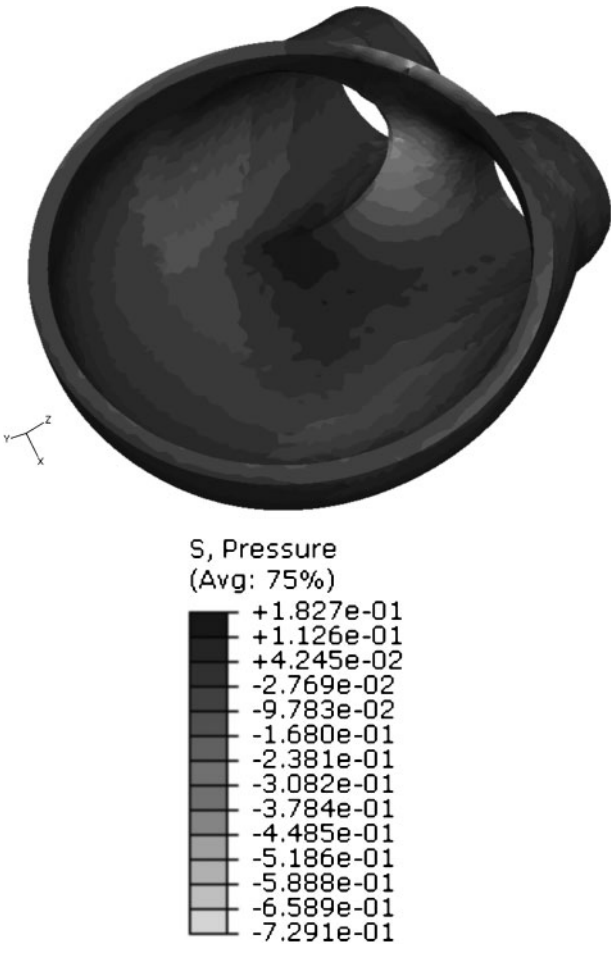

4 Distribution of average stress at inner surface of bottom part of chamber (top view of cross-section)[11]

extremely difficult. On the other hand, the standard laboratory procedures, for example, a tensile test, are not performed for thin films.[2] Thus, it was suggested that application of the inverse analysis combined with the nanoindentation test should be the efficient way of identifying material parameters for coating/substrate system. A reliable and robust model of the experiment is essential for accurate solution of the direct problem and successful application of the inverse method. Thus, the sensitivity analysis should be performed to specify the influential input parameters of the FE model of the test, which have to be considered. The authors' developed FE code accounts for the residual stress distribution for coatings in the specimen. This code can be easily connected with the optimisation algorithm required in the inverse procedure.

Experimental

Specimen and material

Lasers can be used to fabricate thin films by condensing the material ablated from a target (with the laser light) on a different substrate surface.[1] Depending on the specific laser and material parameters, ablation takes place under quasi-equilibrium conditions, as in the laser induced thermal vapourisation, or far from equilibrium, as in many cases of pulsed laser ablation. Thin film formation based on pulsed laser ablation is termed PLD. Pulsed laser deposition is of particular interest because it enables one to fabricate multicomponent stoichiometric films from a single target. In the PLD method applied in the present work, the high purity titanium targets were used for the ablation experiments using a pulsed Nd:YAG laser system, which provides four beams of 1064 nm wavelength, 0·6 J pulse energy and 10 ns pulse duration at a repetition rate of 50 Hz. In this multispot evaporation system, the targets were rotated during laser irradiation in order to avoid the formation of deep craters. The emitted species were deposited at room temperature (~25°C).

The TiN/substrate specimen is prepared to be used in the nanoindentation test. The substrate is a typical ferritic steel. The first material layer is a 1·5 mm thick ferritic steel, and the second is a 1 μm thick TiN coating deposited by the PLD method. The thickness of the coating was determined using the profilometer and the rotating ball disc. These two methods were used because of the resolution problems that were observed in investigation of very thin coatings. The results were additionally confirmed by the time, process parameters and number of laser shots with the evaporated material considering estimation.

Justification of the selection of the TiN material is presented briefly below.

Titanium nitride is particularly interesting due to its high wear resistance and good thermal stability associated with high hardness and high corrosion resistance. The use of TiN coating for orthopaedic prostheses, cardiac valves and dental prostheses has been well documented,[12] along with the haemocompatibility of TiN. Thin coatings of TiN can be deposited by a number of processes; however, for example, the polyurethane (PU) substrate cannot withstand the elevated temperature entailed by the methods. Thus, there is a great

Table 1 Titanium nitride mechanical properties[13–17]

Deposition process	Material description	Experimental method	Hardness H, GPa	Young's modulus E_r, GPa	Residual stress, GPa	Reference
Self-propagating high temperature synthesis	Dense and homogeneous bulk substoichiometric titanium nitride, surrounded by a porous stoichiometric titanium nitride	Indentation test	No data	180–260	No data	13
Ion implantation in pure polycrystalline titanium	Substoichiometric titanium nitrides: δ-iN and ε-Ti_2N	Indentation test	20–33	180–270	No data	14
Self-propagating high temperature synthesis and densification by hot pressing without additives	Nanometric powders	Indentation test	18	150–430	No data	15
Radio frequency magnetron sputtering	Compact very thin coatings, structure similar to zone T and zone 1 in the structure zone model[17]	Indentation test and bulge test	12–21	100–600	0·2–0·4 GPa tensile stress for Young's modulus 100–300 GPa and 0·1 GPa compressive stress for Young's modulus 300–600 GPa	16

demand for developing low temperature deposition processes, such as PLD.

According to Refs. 13–17, the following material properties of TiN coating were specified in wide range of values and are briefly presented in Table 1. A literature research dedicated to material properties of examined material and to measured residual stresses was performed. It indicated the necessity of preparing own experimental tests coupled with numerical methods for correct determination of parameters of the material model of TiN coating on the basis of nanoindentation test.

The technical reasons for applying nanoindentation instead of tensile test for coatings are briefly justified below according to Refs. 2 and 18. Tensile tests have the advantage of uniform stress and strain fields, which is why they are mostly used to determine mechanical properties at larger scales. They provide stress–strain curve, and thus, one can measure the mechanical properties easily and reliably. However, they have disadvantages at smaller scales in that larger forces are required and specimen gripping may be difficult. In addition, specimen preparation can be expensive and time consuming. Gripping and alignment are fraught with potential errors. Strain measurement requires unique approaches. The second known method, which is the nanoindentation test, is easy to use and requires little specimen preparation. The principal goal of this testing is to extract elastic modulus and hardness of the specimen material from experimental readings of indenter load and depth of penetration. For these reasons, this method is widely used in testing, especially of thin films up to nanometre scale thickness. On the other hand, there are many factors to consider for extracting quantitatively reliable mechanical properties from a nanoindentation test.

Recapitulating, there is a lack of mechanical properties of TiN coating deposited on elastic substrate using the PLD method. The nanoindentation test is fully recommended to obtain mechanical properties of TiN coatings deposited on substrates by applying different deposition techniques.

Results of the authors' earlier research[12] for TiN, performed to obtain the values of residual stress in TiN after deposition process using PLD method, are shown in Table 2. Dealing with the thickness from 0·5 μm, it needs to be concerned that the coating is deposited with the late mechanism of the thin film growth. Thus, the thicker the coating is, the lower are the residual stresses.

The crystalline phases present in the TiN coatings were studied by means of X-ray diffraction. Crystallographic texture was observed using the same method. The application of a pseudoposition sensitive detector allowed measurement of the macroresidual stress

Table 2 Values of residual stress measured[12] for TiN deposited by PLD method on polyurethane substrate

Number of specimen	Coating thickness, μm	Residual stress (compressive stress), GPa
1	0·5	2·4
2	1	1·7
3	3	1·5

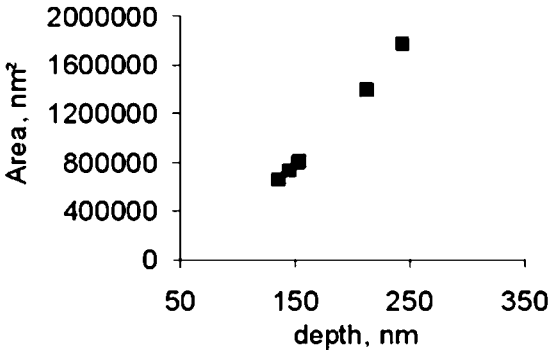

5 Area of indenter versus contact depth for TiN

distribution simultaneously with the crystallographic texture. The layer microstructure was investigated with a transmission electron microscope. Application of the scratch technique allowed observation of the top view of the columns of the layer. A comparison of TiN results between Refs. 13–16 and the authors' data leads to a conclusion that the values of compressive residual stresses are bigger when TiN is deposited by PLD method. Therefore, the compressive residual stress distribution obtained by the authors[12] was introduced as the initial stress in the mathematical model of specimen deformed during the nanoindentation test in the present work.

Nanoindentation test: experimental procedures and data processing

The application of nanoindentation test allows exact determination of hardness and elastic modulus of thin films of a minimal film thickness equal several tens of nanometres, without noticeable influence of the substrate hardness. The technique is based on indenting of the indenter, which is pressed into the surface with the forces in the range from nanonewton to micronewton. As it is done in the universal hardness tests, nanoindentation depth is measured simultaneously. The Berkovich indenter made of diamond is used. The indenter has a top angle of 142·3°, which makes it usable for thin films of >100 nm thickness. The very low indentation depth allows fulfilling the requirement of the standards of a maximum of one-seventh of the indentation depth/film thickness ratio. Larger indentation depths would result in plastic zone formation not only in the film but also in the interface and in the substrate material.

The hardness H and elastic modulus E are measured in the paper on the basis of the elastic contact problem of Boussinesq and Hertz from the measured force/indentation depth ratio of a measuring cycle of loading and unloading. The slope of the loading curve increases with increasing indentation depth h (due to the increasing contact area between the film and indenter). When the force maximum is reached, further deformation due to plastic flow during 30 s waiting at this force is seen. The hardness of the material is calculated from the equation

$$H = \frac{P_{\max}}{A_{\max}} \tag{1}$$

where $A_{\max}$ is the maximal projected contact area and $P_{\max}$ is the maximal indentation force.

The calibration of the tip shape is based on the determination of the shape function of the indenter.[2]

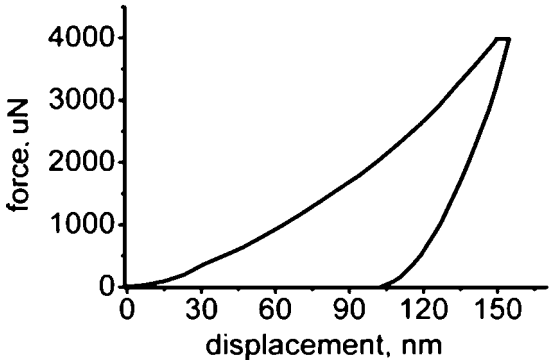

6 Force–displacement curve measured for TiN

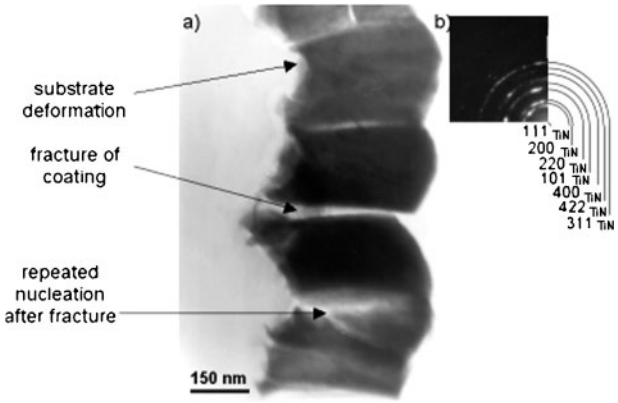

7 *a* microstructure (TEM) of 350 nm TiN coating deposited on polyurethane and *b* electron diffraction computed using program described in Ref. 19

This method assumes that Young's modulus is constant and independent of indentation depth. Fused quartz with Young's modulus of 72 GPa is used as a standard sample for calibration purposes. The shape function is obtained in the relation between the projected contact area A and the contact depth h_c. For an ideal geometry of pyramidal tip (Berkovich indenter), the projected contact area is related to the depth and given by equation

$$A = 24{\cdot}5h_c^2 \tag{2}$$

Equation (2) is a result of approximation of experimental results obtained by the authors and shown in Fig. 5. The shape of the indenter introduced into the FE code is based on results of experimental calibration related to contact area A and contact depth h_c. The experimental function is called the shape function and describes area A for the investigated TiN/ferritic steel specimen. This function gives good accuracy for larger distance from the tip and should not be used very close to the tip. Based on the authors' earlier results, a certain and acceptable FE model assumption related to the shape of indenter is made. The indenter is not a pyramid but is a cone; the contact area A and contact depth h_c are taken from experimental studies. The full description of FE model assumptions is presented in the modelling part of the present paper.

The initial, unloading contact stiffness S is determined by slope of initial part of the unloading part of indentation curve, as follows

$$S = \frac{\mathrm{d}P}{\mathrm{d}h} = \frac{2E_r A^{1/2}}{\pi^{1/2}} \tag{3}$$

where h is the depth and P is the unloading (force).

Transformation of equation (2) gives

$$A = \frac{\pi}{4}\left(\frac{S}{E_r}\right)^2 \tag{4}$$

where E_r is the reduced Young's modulus calculated by assuming that the measured depth includes contribution of both the specimen and the indenter

$$\frac{1}{E_r} = \left(\frac{1-\nu_s^2}{E_s}\right) + \left(\frac{1-\nu_i^2}{E_i}\right) \tag{5}$$

where E_s and E_i are the Young's moduli, and ν_s and ν_i are Poisson's ratios of the specimen and the indenter respectively.

An atomic force microscope with a nanoindenter (TriboScope, Hysitron, Minneapolis, MN, USA) is used in the present work. The maximal force set to specimen using Berkovich indenter was 11 mN. Loading and unloading velocity was 20 nm s^{-1} with 30 s holding time at the maximum force. According to the most popular MatWeb material property data,[13–16] and considering the known book,[2] the following intervals of the frequently measured properties of analysed coating are assumed in Table 3 for wide range of deposition processes. These values can vary for different deposition processes, which is precisely shown in Table 1.

The properties obtained in nanoindentation performed in the present paper are also shown in Table 3 and compared with data observed in literature. The biggest difference is noticed for the measured hardness, which is smaller for the tests in the present work. This difference is attributed to the type of deposition process and substrate material. In the present work, thin film is deposited by the PLD method.

The force–displacement data measured in nanoindentation test for TiN coating/ferritic steel are presented in Fig. 6. The observations made on the basis of the results of nanoindentation test allow expecting the elastic–plastic properties of TiN coating and, therefore, confirming purposefulness of identifying the parameters in material models of coatings by inverse procedure.

Transmission electron microscopy microstructure of TiN coating deposited on PU

Transmission electron microscopy was adopted to analyse the TiN coating. The examined coating of 0·35 μm was assumed to be representative for 'thick'

Table 3 Intervals of TiN properties observed in literature for different deposition processes and measured by authors

Source	Hardness, GPa	Young's modulus E_r, GPa	Poisson's ratio
Literature	12–33	100–600	0·25
Authors	6·04	155	0·25

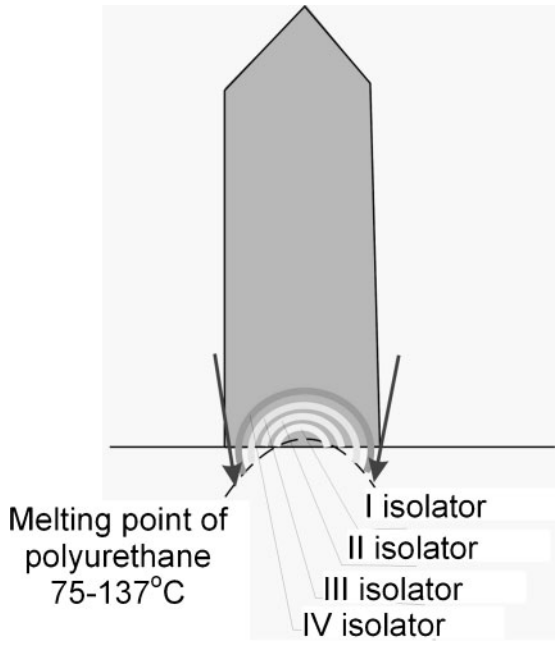

8 Suggestion of interpreting formation of columnar structure of coating and substrate deformation

coatings and thinner than the coatings, which have been investigated until now by the authors. The specimens of TiN cross-sections equal to 0·35 μm deposited on PU substrate were prepared using microtome technique. The TEM research proved the occurrence of substrate deformation during deposition, coating fracture or its 'bridge' effect and repeated nucleation of coating growth after fracture (see Fig. 7).

The formation of characteristic columns proves the formation of coating by the late growth mechanism, called columnar mechanism.[19] Polyurethane is a copolymer, and the contribution of elastic segments varies in dependence to temperature. The early stages of deposition process may lead to formation of isolators, which have an influence on substrate deformation (compare Fig. 8). The observed coating behaviour is an effect of late mechanism of deposition.

Finite element model

Assumptions

Finite element simulations of nanoindentation test for system of coatings face difficulties, which are due to the

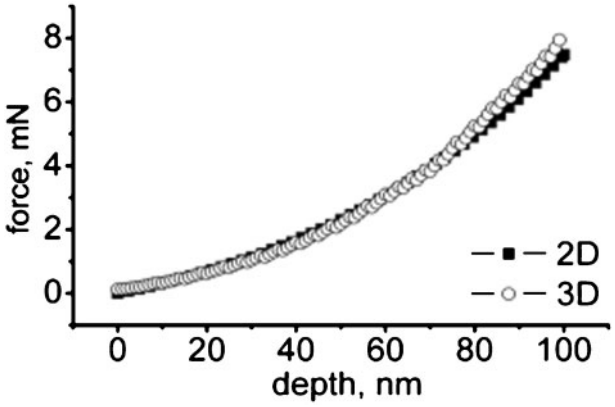

9 Comparison between output of 2D and 3D models

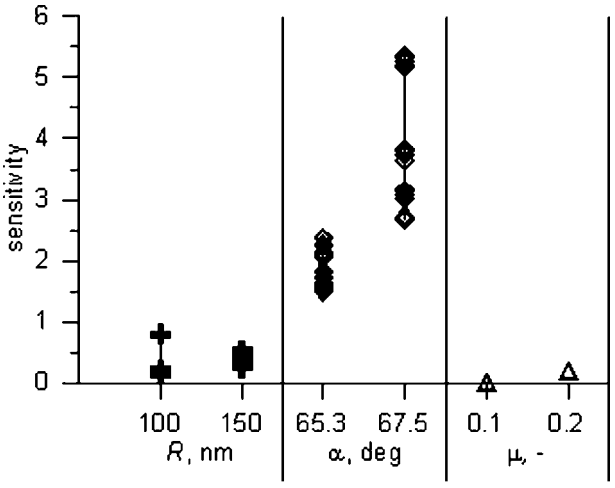

10 Sensitivity with respect to geometrical tip parameters R and α, and friction coefficient μ

thickness of coatings, need of remeshing and scaling procedures as well as the multimaterial and multistage character of simulation. These specified difficulties lead to such inconveniences as a necessity of rescaling, long computing time, necessity of generation of the fine mesh through the thickness for numerous coatings of the system, fine mesh in the region of contact between the small tip of the indenter and comparatively big specimen. The method of overcoming all these difficulties is presented in earlier work.[6]

The basic assumptions in the FE model of nanoindentation test are based on previous investigations[6,7,20] and literature studies.[3–5,21–24] On the basis of the FE simulations using commercial code (Forge 2 and 3),[20] the new model of the test is developed. The distribution of the initial stress assumed as the residual stress and the exact reproduction of the unloading stage, which is the inseparable part of each deformation during nanoindentation test for coatings, are the new capabilities of the model. Beyond this, the open code can be easily connected with the optimisation algorithm, which is indispensable in the inverse approach. The simplifications introduced in the model, which considerably decrease the computational cost, are the following:

(i) approximation of the shape of the Berkovich indenter by a cone
(ii) two-dimensional (2D) axisymmetric solution instead of 3D.

To decrease the computing costs, the simplified 2D axisymmetric model of the nanoindentation test was considered, and the Berkovich indenter was treated as a conical one. Such simplified model does not cause lost of important information, which was validated through the full 3D FE model simulation of nanoindentation tests.[20,21] The results of the comparison of 2D simulation and the full 3D model obtained by the authors of the present work are shown in Fig. 9.[20]

In addition, the authors calculated the sensitivities of the nanoindentation test with respect to the Berkovich indenter shape parameters R and α, and friction coefficient μ (compare Ref. 20 and Fig. 10). The results of the sensitivity analysis show that the nanoindentation test is the most sensitive to the geometrical parameters of the tip.

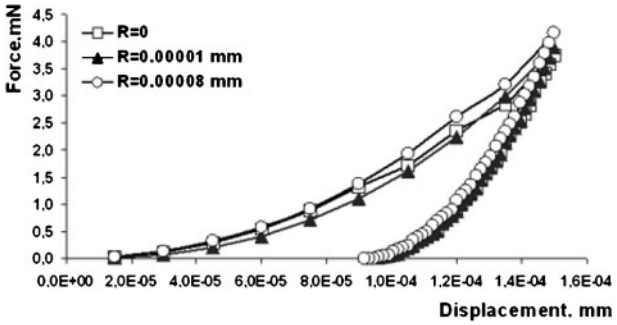

11 Relation between force and displacement for three radii of spherical tip of indenter

Thus, the present study checked the influence of spherical tip of the indenter on the model output. Three different radii of tip were analysed: 0·0, 0·00001 and 0·00008 mm. The relation between force and displacement were obtained and presented in Fig. 11. The differences among FE model outputs were not significant, especially considering big disturbances of tip radii. Therefore, the authors assumed that the spherical tip of the indenter can be neglected in further studies. In addition, the results of distribution of effective strain (see Fig. 12) are also not significantly disturbed by the spherical tip of indenter; only very small differences were observed. Recapitulating, the effect of the spherical tip of the indenter is not worth to be introduced in the new models of nanoindentation test because of very small influences on force–displacement data.

The further work was dedicated to the sensitivity analysis with respect to the shape parameter (angle α) of the cone indenter (modelled version of Berkovich indenter), which is presented in Ref. 21. The sensitivity analysis of the model of the nanoindentation test, with respect to the wide range of cone indenter angles, leads to the conclusion that this sensitivity varies for different angles. The maximum value of the sensitivity is observed for an angle of 58°, while the smallest is observed for an angle of 88°. In comparison, the sensitivity obtained for the angle 70° of the indenter (nominal Berkovich indenter) is a medium sized value. Computed stress distributions in the specimen show that the cone indenter with an angle of 70° introduces the smallest values of stress. Therefore, the model of indenter with an angle of 70° was selected by the authors and was applied in the present paper.

Numerical tests for the specimen composed of coatings confirmed good compatibility between Forge 2 and the authors' FE codes for the loading stage, as shown in Fig. 13.

The lack of the uniqueness of the inverse analysis was the disadvantage of the previously selected Hollomon material model.[7] It was impossible to find out precisely, without additional experimental data (the tension test data was used in Ref. 7), which combination of parameters in the applied model was the best solution of the defined inverse problem. In addition, the Hollomon model does not allow determining the exact point (values of stress and strain), in which the plastic part of material model is reached during deformation. The latter fact is important due to application of analysed coatings, which cannot be deformed plastically (irreversibly). Therefore, the bilinear material model of coating in the constitutive law is assumed in the present work. This model is expressed by the following equations

$$\sigma_{\mathrm{i}} = E\varepsilon_{\mathrm{i}} \text{ if } \sigma_{\mathrm{i}} \leq Y \tag{6}$$

$$\sigma_{\mathrm{i}} = Y + \beta(E\varepsilon_{\mathrm{i}} - Y) \text{ if } \sigma_{\mathrm{i}} > Y \tag{7}$$

where σ_{i} is the intensity of stress, ε_{i} is the intensity of strain, E is the Young's modulus, Y is the yield stress and β is the hardening coefficient ($0 \leqslant \beta \geqslant 1$; $\beta=1$ for ideal elastic materials, $\beta=0$ for ideal plastic materials).

This bilinear elastic–plastic material model assumed for TiN coating is plotted in Fig. 14. The parameters ε_1, ε_2, σ_1 and σ_2 in the model have to be determined using inverse analysis.

Basic equations

The initial stress $\{\sigma_{0\ \mathrm{res}}\}$ is taken into account in the formulation of boundary problem. The relation between stresses and strains[23] is written using the matrix form

$$\{\sigma\} = [D](\{\varepsilon\} - \{\varepsilon_{0\ \mathrm{res}}\}) \tag{8}$$

where

$$\{\varepsilon_{0\ \mathrm{res}}\} = \begin{Bmatrix} \varepsilon_{0\ \mathrm{res}} \\ \varepsilon_{0\ \mathrm{res}} \\ \varepsilon_{0\ \mathrm{res}} \\ 0 \end{Bmatrix} \tag{9}$$

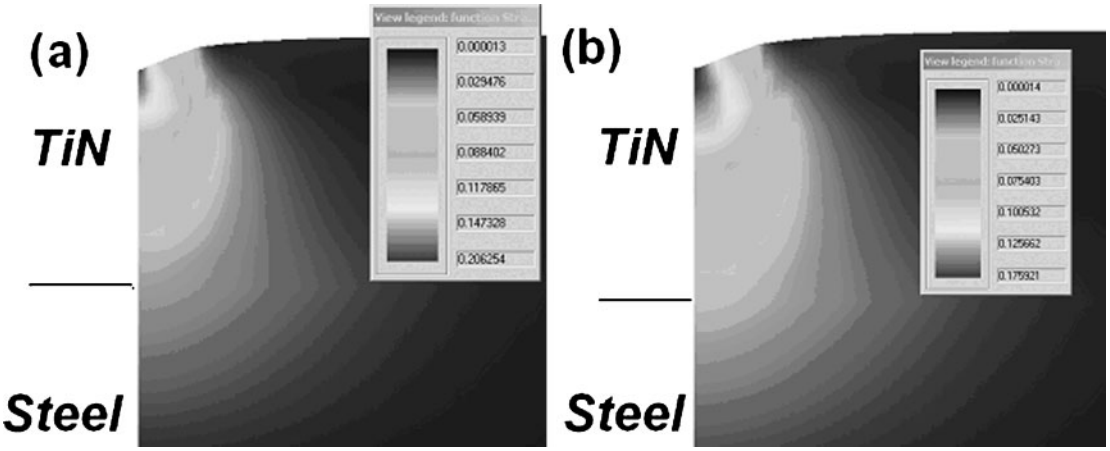

a $r=0$ mm; *b* $r=0{\cdot}00008$ mm

12 Distribution of effective strain for two radii of spherical tip of indenter

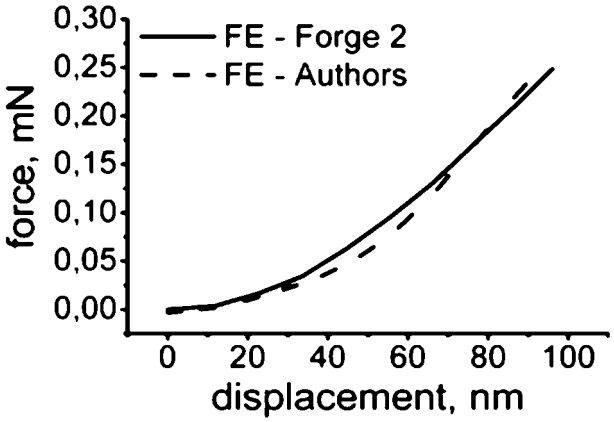

13 Comparison between output predicted by Forge 2 and authors' code

$$[D]=\frac{E'}{(1+\nu)(1-2\nu)}\begin{bmatrix}1-\nu & \nu & \nu & 0\\ \nu & 1-\nu & \nu & 0\\ \nu & \nu & 1-\nu & 0\\ 0 & 0 & 0 & (1-2\nu)/2\end{bmatrix} \tag{10}$$

$$E'=\frac{\sigma_{\mathrm{i}}}{\varepsilon_{\mathrm{i}}} \tag{11}$$

where $\{\sigma\}=\{\sigma_{\mathrm{r}}\ \ \sigma_{\mathrm{z}}\ \ \sigma_{\theta}\ \ \tau_{\mathrm{rz}}\}^{\mathrm{T}}$ is the stress tensor in the cylindrical coordinate system, $\{\varepsilon\}=\{\varepsilon_{\mathrm{r}}\ \varepsilon_{\mathrm{z}}\ \varepsilon_{\theta}\ 2\varepsilon_{\mathrm{rz}}\}^{\mathrm{T}}$ is the strain tensor in the cylindrical coordinate system, ν is the Poisson's ratio, $\{\sigma_{0\ \mathrm{res}}\}$ is thee initial (residual) stresses, $\{\varepsilon_{0\ \mathrm{res}}\}$ is the initial (residual) strains, which are independent of stresses $\{\sigma\}$, and E' is the modulus of plasticity, which is equal to Young's modulus in elastic zone in linear elasticity (see equation (6)). For linearisation of boundary problem, the method of iterative calculation of modulus of plasticity is used.

The variational principle of the non-linear elastic and elastic–plastic theory leads to the following functional form for FE e

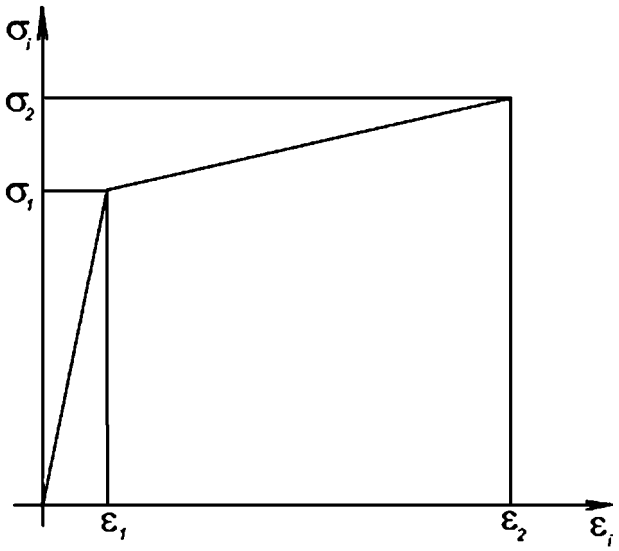

14 Hardening curve of coating

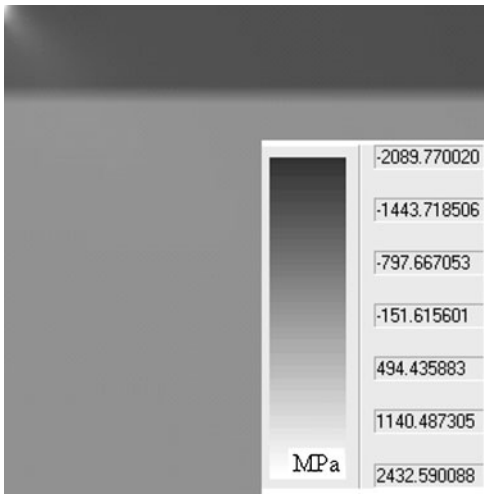

15 Residual stress distribution in TiN/steel specimen

$$W_{\mathrm{e}}=\int_{V_{\mathrm{e}}}\frac{1}{2}\{U\}^{\mathrm{T}}[B]^{\mathrm{T}}[D][B]\{U\}\mathrm{d}V-\int_{V_{\mathrm{e}}}\{U\}^{\mathrm{T}}[B]^{\mathrm{T}}[D]\{\varepsilon_{0\ \mathrm{res}}\}\mathrm{d}V-\int_{S_{\mathrm{e}}}\{U\}^{\mathrm{T}}[\bar{N}]^{\mathrm{T}}\{p\}\mathrm{d}S \tag{12}$$

where S is the contact surface between material and indenter, $\{p\}$ is the contact stress, $\{U\}$ is the displacement vector, $[B]$ is the matrix containing the derivations of shape functions, $[D]$ is the matrix containing the appropriate material properties in equation (10), $[\bar{N}]$ is the matrix of shape functions of FE, V is the volume of sample, V_{e} is the volume of current FE e, S_{e} is the contact surface between current outside element e and surface of indenter.

The stiffness matrix $[K]$ and load vector $\{F\}$ are written according to forms

$$[K]=\int_{V_{\mathrm{e}}}[B]^{\mathrm{T}}[D][B]\mathrm{d}V \tag{13}$$

$$\{F\}=-\int_{V}[B]^{\mathrm{T}}[D]\{\varepsilon_{0\ \mathrm{res}}\}\mathrm{d}V \tag{14}$$

The initial stress (residual stress) distribution has to be specified for each element of FE model mesh in the beginning stage of solution process. The next stage is based on the inverse idea. The collocated distribution of $\varepsilon_{0\ \mathrm{res}}$ is determined based on the minimisation of the following function

$$R=\sum_{e=1}^{N_{\mathrm{e}}}\int_{V_{\mathrm{e}}}[\sigma_{0\ \mathrm{res}}(\varepsilon_{0\ \mathrm{res}})-\bar{\sigma}_{0\ \mathrm{res}}]^2\mathrm{d}V \tag{15}$$

where e is the number of current FE, N_{e} is the number of FEs in zone with initial stress, $\bar{\sigma}_{0\ \mathrm{res}}$ is the experimental value of initial stress in current FE e, and $\sigma_{0\ \mathrm{res}}(\varepsilon_{0\ \mathrm{res}})$ is the calculated distribution of initial stresses dependent of $\varepsilon_{0\ \mathrm{res}}$. In the present work, the value of $\bar{\sigma}_{0\ \mathrm{res}}$ is equal to 1·5 GPa (see Table 2). The value of initial stress is taken from Ref. 12 and, in the present work, is interpreted as

mean stress

$$\sigma_{0\ \mathrm{res}} = \frac{\sigma_\mathrm{r} + \sigma_\mathrm{z} + \sigma_\theta}{3} \tag{16}$$

This value is localised in thin TiN coating. After determination of distribution of $\varepsilon_{0\ \mathrm{res}}$ and $\sigma_{0\ \mathrm{res}}$, the simulations of loading and unloading stages are possible. The residual stress distribution in the TiN/steel specimen is presented in Fig. 15. There are two fine mesh areas in the FE model of this specimen. They are located in the upper coating and in the centre of the specimen. The FE model, which is used to solve the boundary problem, is composed of 3689 four-node FEs and 3840 nodes. The average computing time of the complete two-stage simulation (40 computing steps) using standard PC is ~0·3 h. Using the commercial FE code (Forge code) increases the computational cost about several times.

Modelling of the unloading step is performed following the theorem of unloading introduced in Ref. 23. The following algorithm is performed for each time step of unloading:

(i) the distributions of stresses $\{\sigma\}$ and strains $\{\varepsilon\}$ before unloading are the solutions of the problem for active loading
(ii) the specimen is loaded by the inverse force, and the material is modelled as an elastic; the fields of $\{\sigma^\mathrm{e}\}$ and $\{\varepsilon^\mathrm{e}\}$ are obtained after this procedure
(iii) the actual state of stress and strain during the unloading stage is reached as the sum of the following solutions

$$\left\{\sigma^{\mathrm{unload}}\right\} = \{\sigma\} + \{\sigma^\mathrm{e}\} \tag{17}$$

$$\left\{\varepsilon^{\mathrm{unload}}\right\} = \{\varepsilon\} + \{\varepsilon^\mathrm{e}\} \tag{18}$$

where $\{\varepsilon^\mathrm{e}\}$ is the elastic part of strain and $\{\sigma^\mathrm{e}\}$ is the elastic part of stress.

Sensitivity analysis

The design of conditions of an effective nanoindentation test and an adequate choice of the key parameters of the FE model are usually preceded by the sensitivity analysis. This analysis is used to determine the important process parameters, which control the mechanical response of the modelled process, and to design the optimum values of these parameters. The algorithm described in Ref. 25 is used. Moreover, sensitivity analysis specifies how and to what extent modifications of the model input data influence specified output data.

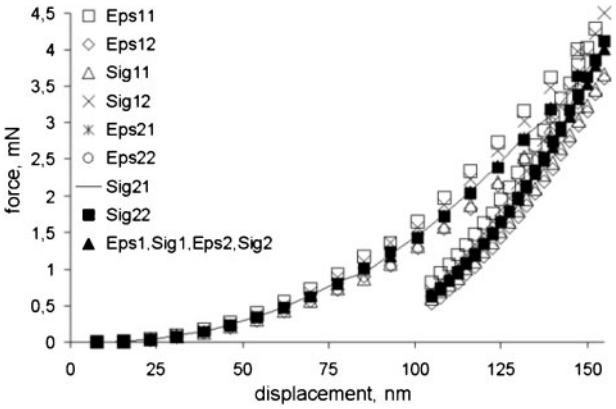

16 Results of 1–8 simulations for disturbed parameters of TiN material models

Sensitivity coefficients

Sensitivity analysis allows estimation of the influence of the individual process parameter on the value of the analysed one. The considered parameter is the total load in the nanoindentation test; therefore, the sensitivity of the work with respect to the selected process parameter is determined. The sensitivity with respect to the parameter numbered as j (φ_{pj}) at the point $\mathbf{p}^*$ is defined as

$$\varphi_{\mathrm{p_j}}\Big|_{\mathbf{p}^*} := \frac{p_\mathrm{j}^*}{W(\mathbf{p}^*)} \left.\frac{\partial W}{\partial p_\mathrm{j}}\right|_{\mathrm{p}^*} \cong \frac{p_\mathrm{j}^*}{W(\mathbf{p}^*)} \frac{W(\mathbf{p}^* + \Delta p_\mathrm{j}\mathbf{e}_\mathrm{j}) - W(\mathbf{p}^*)}{\Delta p_\mathrm{j}} \tag{19}$$

where $\mathbf{p}^* = (\varepsilon_1^*, \varepsilon_2^*, \sigma_1^*, \sigma_2^*, \sigma_{\mathrm{res}}^*, d^*)$ is the considered point in the space of parameters ε_1, ε_2, σ_1 and σ_2 of the material model, σ_{res} is the residual stress, d is the thickness of coating, $\mathbf{e}_\mathrm{j}$ is the vector of the canonical basis, Δp_j is the variation of the parameter p_j and W is the average total work, calculated as follows

$$W = \int_0^{\mathrm{h_f}} \mathrm{F}(h)\,\mathrm{d}h \tag{20}$$

where $\mathrm{F}(h)$ is the load and h_f is the total displacement of the process.

The sensitivities of the work with respect to the parameters of the material model (ε_1, ε_2, σ_1, σ_2), residual stress in the coating σ_{res} and thickness of coating d are analysed. In the sensitivity procedure, the value of each

Table 4 Parameters of TiN bilinear material model used in sensitivity procedure

	Parameters of material model			
	ε_1	σ_1, MPa	ε_2	σ_2, MPa
Initial values	0·009	2614	0·166	9107
Simulations with disturbed parameters				
Eps11	0·007	2614	0·166	9107
Eps12	0·011	2614	0·166	9107
Sig11	0·009	2353	0·166	9107
Sig12	0·009	2875	0·166	9107
Eps21	0·009	2614	0·149	9107
Eps22	0·009	2614	0·182	9107
Sig21	0·009	2614	0·166	10018
Sig22	0·009	2614	0·166	8196

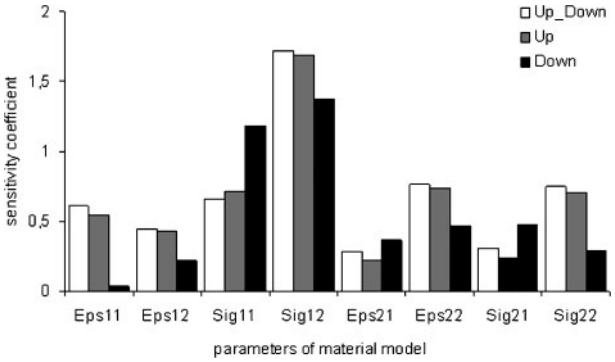

17 Sensitivity coefficients with respect to material model parameters

considered parameter is disturbed by 10% with respect to its initial value in the study.

Results of sensitivity analysis and discussion

To estimate the effect of chosen bilinear material model for TiN coating on the output of the FE model, the simulations for the data presented in Table 4 are performed.

Force–displacement curves for the data in Table 4 are plotted in Fig. 16. The sensitivity coefficients determined using equations (19) and (20) are shown in Fig. 17. The difference between loading and unloading stage of nanoindentation test is clearly visible in this figure. The whole response of the FE model is referred to as 'Up_Down'. The partial response related to loading stage is called 'Up', and the part responsible for the unloading stage is called 'Down'. The contribution of the unloading phase into the sensitivity coefficients is smaller than that of the loading phase. The general conclusion is that all sensitivity coefficients are small. The biggest value of this coefficient is obtained for 'Sig12'. The average sensitivity coefficient with respect to the parameters of TiN bilinear model is 0·5.

The thickness of the deposited TiN coating is the dependent variable in the second step of the sensitivity analysis. The three thicknesses were examined: 0·0009 mm, 0·001 mm and 0·0011 mm. Force–displacement curves for these three thicknesses are plotted in Fig. 18. The sensitivity coefficients calculated with respect to thickness of TiN are shown in Fig. 19. The contribution of unloading phase into the sensitivity coefficients is, in this case, similar to the contribution of the loading phase. The values of the sensitivity

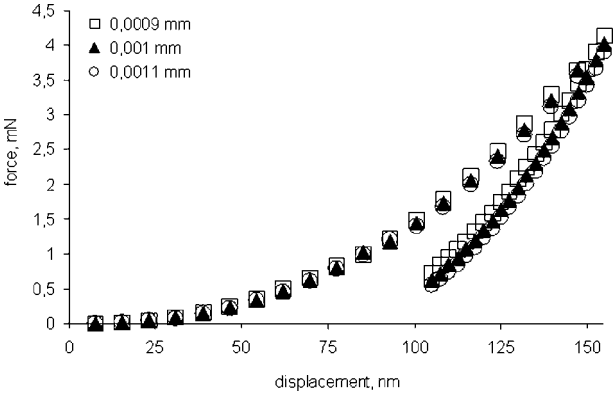

18 Results of simulations for disturbed thickness of TiN coating

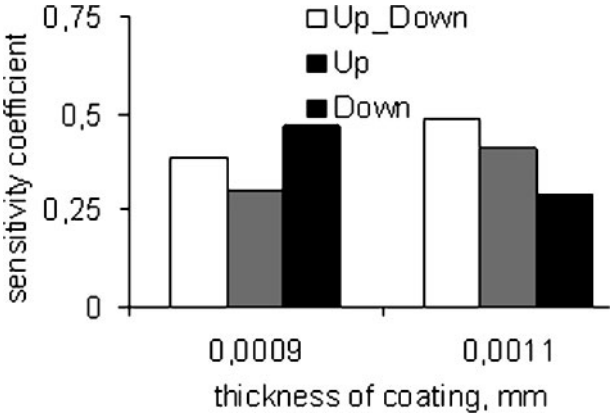

19 Sensitivity coefficients with respect to thickness of TiN coating

coefficients are small, and the average value of this coefficient is 0·5.

The last step of the sensitivity analysis was dedicated to evaluation of influence of residual stress. Three residual stresses were considered: 1·35 GPa, 1·5 GPa and 1·65 GPa. The force–displacement curves corresponding to these stresses are plotted in Fig. 20, and the calculated sensitivity coefficients are shown in Fig. 21. The contribution of unloading phase into the sensitivity coefficients is, in this case, significantly bigger in comparison with the loading phase. The values of sensitivity coefficients are very small and the average value of this coefficient is 0·15. Therefore, there is no need for high precision of evaluation of the residual stresses.

Inverse analysis

The purpose of this part of the work was the identification of the material model parameters on the basis of the nanoindentation test data for biocompatible coating deposited on substrate. The known analytical methods described in Ref. 2 used in experimental nanoindentation test lead to the evaluation of material properties, and they give good results for the basic material parameters (Young's modulus and hardness) but not for the complete material models.

In the previous work,[7] the conformity between the inverse approach for indentation and the tension test for

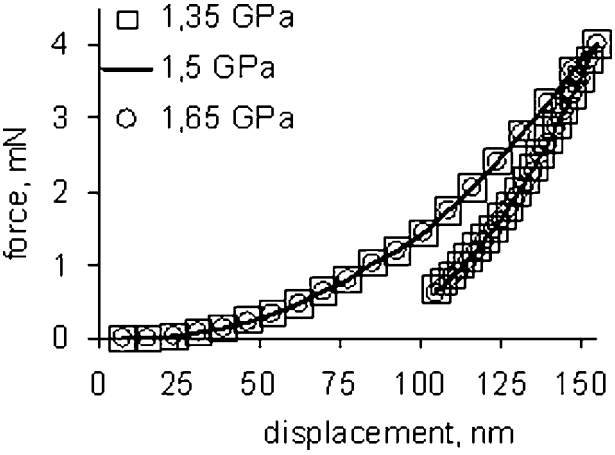

20 Results of simulations for disturbed residual stress of TiN coating

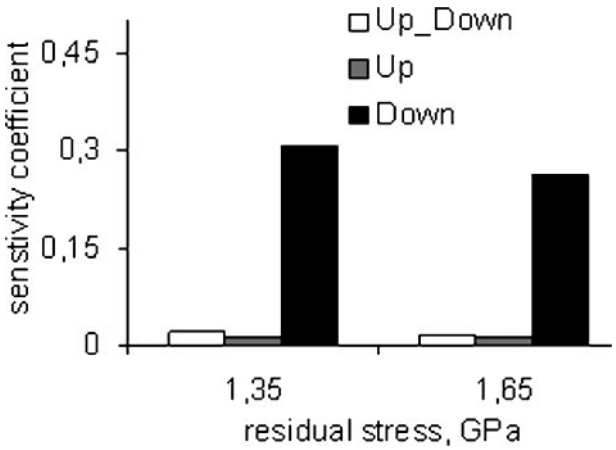

21 Sensitivity coefficients with respect to residual stress of TiN coating

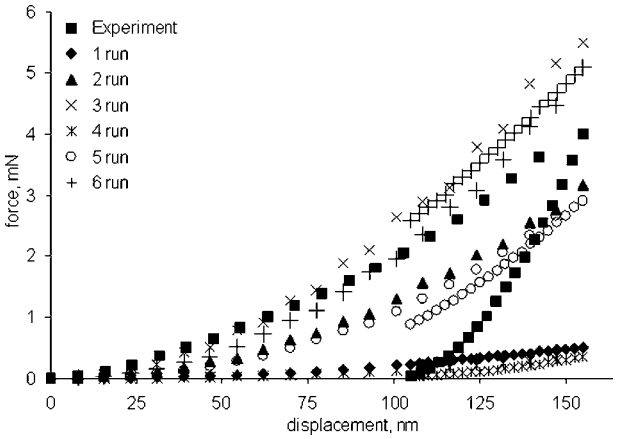

23 Outputs of model: inverse results of 1–6 computing runs for 1–6 starting points

the steel specimen was investigated because the latter experiment gives more consistent results. However, this test cannot be performed for coatings. However, the good capability of the inverse method to determine the parameters for the material model of C–Mn steel was confirmed, and, therefore, this method is used in the present work to identify parameters of material model for TiN coating using the nanoindentation test results.

Description of method

The idea of the inverse analysis presented in Fig. 22 is to find, using the optimisation procedure, the parameters of material model, which give the best matching between results of the FE simulation and experiment. In the considered case, the specified goal function in optimisation is the mean square root error between measured and predicted loads in the nanoindentation test

$$\varphi = \left[\frac{1}{N} \sum_{i=1}^{N} \left(F_{EXP}^{i} - F_{SIM}^{i} \right)^2 \right]^{1/2} \tag{21}$$

where F_{EXP} is the experimental forces versus depths, F_{SIM} is the values of forces versus depths predicted by the FE model and N is the number of sampling points in each test.

The output of simulation is force versus depth data at the loading and unloading stages of the nanoindentation test. In the present work, the number of sampling points N is equal to 40 for both simulation and experiment, 20 sampling points for loading and 20 points for the unloading phase. Optimised variables are σ_1, ε_1, σ_2 and ε_2 in the bilinear elastic–plastic material model for the TiN coating, described by equations (6) and (7). These parameters are determined by searching for the minimum of the goal function (21). Stop criterion is achieved if the predicted value of force for the indented specimen is close enough to the experimental one.

The inverse solution used the simplex optimisation method.[7,26] Each evaluation of the goal function requires FE simulation, which approximately lasts ~10 h. Thus, to decrease the computing cost, the penalty functions are applied for the forbidden intervals of material model parameters.

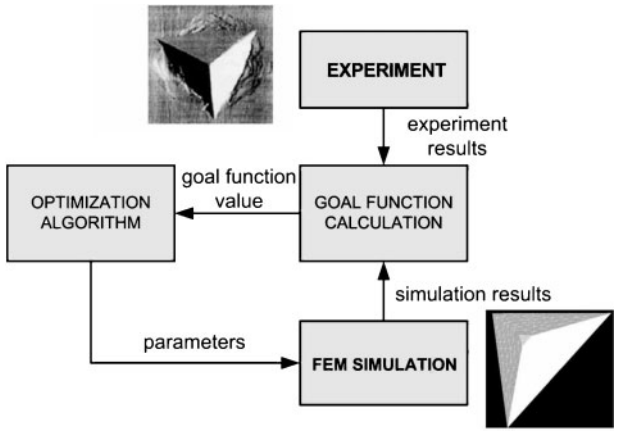

22 Flow chart of inverse analysis

Results and discussion

The whole inverse analysis for the nanoindentation test of investigated TiN/ferritic steel specimen lasts a few days. The value of goal function was large in most of the performed computing runs, but the finally achieved result considered as the set of parameters of material model is related to the smallest value of goal function. The computed results are shown in Figs. 23–26 for comparison with experimental data, not only considering the small value of the goal function. The analysis and comparison done among all calculated results lead to the statement that the result of the computing run no. 9 gives the best match between numerical and experimental data using developed FE model and code.

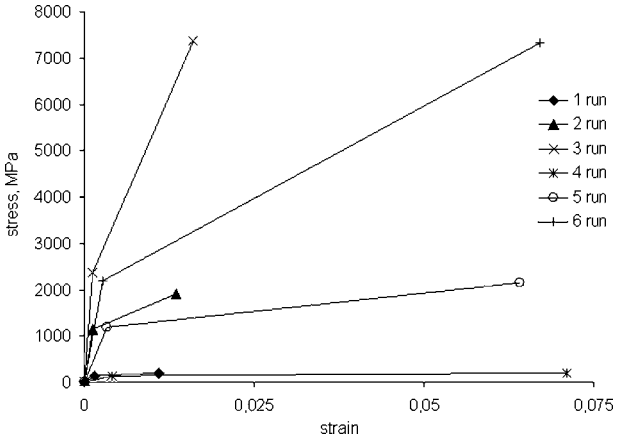

24 Material models: inverse results of 1–6 computing runs for 1–6 starting points

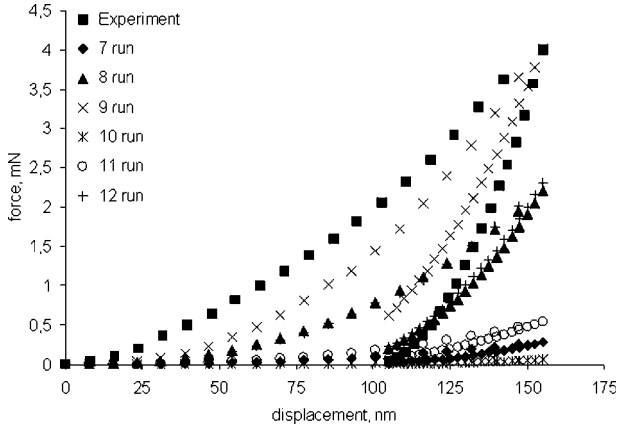

25 Outputs of model: inverse results of 7–12 computing runs of 7–12 starting points

What's more, the predicted value of maximum force for the indented specimen is equal to the experimental one, and the goal function reaches the minimum. Thus, the parameters of chosen material model for TiN deposited on ferritic steel are as follows: $\varepsilon_1=0{\cdot}009$, $\sigma_1=2614$ MPa, $\varepsilon_2=0{\cdot}166$ and $\sigma_2=9107$ MPa. According to this solution, the elastic modulus of TiN is equal to 290·4 GPa. The obtained elastic modulus is also observed in ranges of values given in literature.[2,15,16]

It can be concluded that the bilinear material model does not introduce the lack of uniqueness in solution because only one set of parameters gives the minimum of the goal function. The inverse procedure enables determination of parameters of the material model for coatings using the nanoindentation test data. In addition, the mathematical model of nanoindentation test with initial (residual) stress distribution reproduces the experimental conditions, quite adequately describes the behaviour of the investigated specimen and allows to obtain the satisfying results in a reasonably short time.

Final remarks and prospects

The sensitivities of the output of nanoindentation test model with respect to the thickness of deposited coating, residual stress and parameters of the bilinear material model are presented. The results of the sensitivity analysis unequivocally proved that small disturbances of parameters do not have high influence on model output. The biggest sensitivity coefficient was obtained for parameter σ_1 of the material model. Small changes of the residual stress distribution and coating thickness do not have a significant effect on the model output, but they cannot be totally omitted in the future studies. Beyond this, all parts of simulated deformation process are important in modelling because observed differences between contributions of loading and unloading into sensitivity results are meaningful. The contribution of each stage of deformation is different in different simulations and depends mainly on the parameters of the model. The residual stress is the most influential parameter because it introduces the biggest difference between contribution of loading and unloading stage.

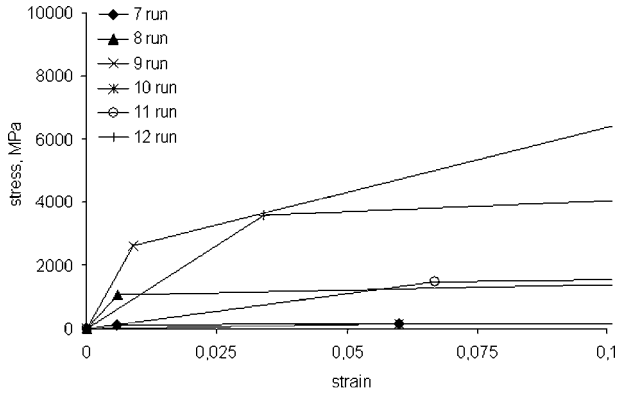

26 Material models: inverse results of 7–12 computing runs for 7–12 starting points

The authors' FE code used in the present paper is capable to reconstruct the unloading part of the nanoindentation curve and to account for the influence of the initial stress distribution. These problems are limitations when the standard commercial FE code is used. However, even when the developed code is used, the computing costs of simulations of the nanoindentation tests repeatedly called in the inverse procedure are very high. Therefore, an additional study dedicated to the development of the efficient optimisation procedure using simplex algorithm and penalty functions was performed.

When the optimal coefficients are introduced in the model, a quite good conformity is observed between the results of the FE simulation and the experimental data. The final value of the goal function (21) is not given because this value is multiplied by penalty functions. On the contrary, the uniqueness of the solution is the advantage of the chosen bilinear material model, which was not noticed for the Hollomon material model used in Ref. 7.

Identification of the material properties for the coatings deposited by PLD technique, which are supposed to be used for artificial heart prosthesis as constructional materials, can be one of the possible future applications of the developed numerical tool. Since good capabilities of the approach used in the present paper was confirmed, the authors intend to use this approach to determine the values of more parameters in the complex material models, even for multilayer coatings, like for example parameters of fatigue material models.

Conclusions

The performed research and achieved results lead to the following conclusions.

1. The conformity between the authors' FE code and the commercial Forge 2 code in the range of deformation during the loading stage in the deformation process is acceptable.

2. The sensitivity analysis of the load in the model of the nanoindentation test, with respect to the parameters of the material model for TiN, residual stress in the coating and thickness of the coating shows that sensitivity is highest for the σ_1 material model parameter. This parameter determines the transition point between elastic and plastic part of the model. Sensitivity with respect to residual stress is larger during unloading stage than during loading. Owing to low values of sensitivities, the need for precise evaluation of the residual stress and thickness of coating measured in experiments is not so restrictive, but they have to be considered and cannot be omitted in future works.

3. The developed model reproduces well the experimental conditions and the behaviour of the investigated specimen and allows getting the result in a reasonably short time. Since even the optimisation algorithm requires numerous simulations of the nanoindentation test, the mentioned features are important advantages of the code.

4. The inverse procedure based on the simplex optimisation technique allowed to determine parameters of the material model for TiN coating deposited on steel. The following values of the parameters were obtained: $\varepsilon_1=0{\cdot}009$, $\sigma_1=2614$ MPa, $\varepsilon_2=0{\cdot}166$ and $\sigma_2=9107$ MPa, which lead to Young's modulus of 290 GPa.

5. The uniqueness of the solution inverse and the capability to give the exact values of strain and stress in the transition point between elastic and plastic part of material model are the advantages of the bilinear elastic–plastic material model for coating.

Acknowledgements

Financial assistance of the MNiSzW (project no. N507 136 32/3962) is acknowledged. The Austrian author would like to thank the Austrian Federal Ministry of Traffic, Innovation and Technology, the Austrian Industrial Research Promotion Fund (FFG) in the frame of the Austrian Nanoinitiative program, the Government of Styria, and the European Union in the frame of EFRE for financial support.

References

1. J. M. Lackner: 'Industrially-scaled hybrid pulsed laser deposition at room temperature'; 2005, Kraków, Orekop.
2. A. Fisher-Cripps: 'Nanoindentation'; 2002, New York, Springer-Verlag.
3. E. G. Berasategui, S. J. Bull and T. F. Page: *Thin Solid Films*, 2004, **447–448**, 26–32.
4. T. F. Page and S. J. Bull: *Philos. Mag. Lett.*, 2006, **86**, 5331–5346.
5. S. J. Bull, E. G. Berasetegui and T. F. Page: *Wear*, 2004, **256**, 857–866.
6. M. Kopernik and M. Pietrzyk: *Arch. Metall. Mater.*, 2007, **52**, 299–310.
7. M. Kopernik, M. Spychalski, K. J. Kurzydłowski and M. Pietrzyk: *Mater. Sci. Technol.*, 2008, **24**, 369–375.
8. J. M. Lackner, W. Waldhauser, R. Major, L. Major and B. Major: *Surf. Coat. Technol.*, 2006, **201**, 4090–4093.
9. R. Major, F. Bruckert, J. M. Lackner, W. Waldhauser, M. Pietrzyk and B. Major: *Bull. Pol. Acad. Sci. Technol.*, 2008, **56**, 223–228.
10. M. Kopernik and J. Nowak: *Arch. Mech.*, 2009, **61**, 171–193.
11. A. Milenin and M. Kopernik: *Acta Biomech. Bioeng.*, 2009, **11**, 13–20.
12. R. Major, E. Czarnowska, A. Sowińska, R. Kustosz, J. M. Lackner, W. Waldhauser, M. Woźniak, T. Wierzchoń and B. Major: *e-Polymers*, 2005, **26**, 1–9.
13. D. Carole, N. Frety, S. Etienne-Calas, C. Merlet and R.-M. Marin-Ayral: *Mater. Sci. Eng.*, 2006, **419**, 365–371.
14. M. Guemmaz, A. Mosser and J. Grob: *Appl. Phys.*, 1997, **64**, 407–415.
15. J. Russias, S. Cardinal, J. Fontaine, G. Fantozzi, C. Esnouf and K. Bienvenu: *Int. J. Refract. Met. Hard Mater.*, 2005, **23**, 344–349.
16. O. R. Shojaei and A. Karimi: *Thin Solid Films*, 1998, **332**, 202–208.
17. J. A. Thornton: *J. Vac. Sci. Technol.*, 1974, **11**, 666–670.
18. C. S. Oh, H. J. Lee, S. G. Ko, S. W. Kim and H. G. Ahn: *Sens. Actuator*, 2005, **117**, 151–158.
19. J. E. Greene: 'Multicomponent and multilayered thin films for advanced microtechnologies: techniques, fundamentals and devices'; 1993, Dordrecht, Kluwer Academic.
20. M. Kopernik and D. Szeliga: *Comput. Methods Mater. Sci.*, 2007, **7**, 255–261.
21. H.-J. Albrecht, T. Hannach, A. Häse, A. Juritza, K. Müller and W. H. Müller: *Arch. Appl. Mech.*, 2005, **74**, 728–738.
22. M. Kopernik and A. Milenin: *Steel Res. Int.*, 2008, **79**, 555–562.
23. A. Ilushin: 'Plastichnost'; 1963, Moscow, AN ZSSR.
24. O. C. Zienkiewicz, R. L. Taylor: 'The finite element method'; 2000, London, Butterworth–Heinemann.
25. D. Szeliga: *Comput. Methods Mater. Sci.*, 2005, **5**, 170–178.
26. J. A. Nelder and R. A. Mead: *Comput. J.*, 1965, **7**, 308–313.